



THE UNIVERSITY *of* EDINBURGH

Edinburgh Research Explorer

Refraction and instability of optical vortices at an interface in a liquid crystal

Citation for published version:

Smyth, N & Xia, W 2012, 'Refraction and instability of optical vortices at an interface in a liquid crystal' Journal of Physics B: Atomic Molecular and Optical Physics, vol. 45, no. 16, 165403. DOI: 10.1088/0953-4075/45/16/165403

Digital Object Identifier (DOI):

[10.1088/0953-4075/45/16/165403](https://doi.org/10.1088/0953-4075/45/16/165403)

Link:

[Link to publication record in Edinburgh Research Explorer](#)

Document Version:

Peer reviewed version

Published In:

Journal of Physics B: Atomic Molecular and Optical Physics

Publisher Rights Statement:

© 2012 IOP Publishing Ltd

General rights

Copyright for the publications made accessible via the Edinburgh Research Explorer is retained by the author(s) and / or other copyright owners and it is a condition of accessing these publications that users recognise and abide by the legal requirements associated with these rights.

Take down policy

The University of Edinburgh has made every reasonable effort to ensure that Edinburgh Research Explorer content complies with UK legislation. If you believe that the public display of this file breaches copyright please contact openaccess@ed.ac.uk providing details, and we will remove access to the work immediately and investigate your claim.



Refraction and Instability of Optical Vortices at an Interface in a Liquid Crystal

Noel F. Smyth¹ and Wenjun Xia¹

¹*School of Mathematics and Maxwell Institute for Mathematical Sciences,
University of Edinburgh, Edinburgh EH9 3JZ, Scotland, U.K.*

The refraction of an optical vortex at a nonlinear refractive index interface in a nematic liquid crystal is studied using modulation theory and numerical solutions. It is found that the refraction of an optical vortex differs in fundamental ways from the refraction of an optical solitary wave. This is due to an optical solitary wave having an inherent instability mode which can be triggered if it interacts too strongly with the interface, leading to the break-up of the vortex into solitary waves. Vortex refraction is studied using both an approximate modulation theory, based on an averaged Lagrangian formulation of the governing equations, and numerical solutions. Excellent agreement is found between the approximate analytical theory and numerical solutions.

PACS numbers: 42.65.Tg, 42.70.Df, 05.45.Yv

I. INTRODUCTION

Nematic liquid crystals form an ideal medium in which to study nonlinear optical effects as their “huge” nonlinearity means that such effects occur over millimetre distances for beams of milliwatt power levels [1, 2]. Two, that is $(2+1)$, dimensional solitary waves are stable in a nematic liquid crystal as this medium is what is termed nonlocal, in that the response of the liquid crystal to the optical beam extends far beyond the waist of the beam. This nonlocal behaviour arrests the usual catastrophic collapse [3] of a $(2+1)$ dimensional solitary wave governed by a nonlinear Schrödinger (NLS)-type equation [1, 4, 5]. The behaviour of optical solitary wave beams, termed nematicons, in nematic liquid crystals has been extensively studied since their initial experimental demonstration [2], see, for example, [1, 4, 5] and references in [6]. Much of this work has been driven by the possible applications of nematicons to all optical devices based on nematic liquid crystals [7–16].

As well as optical solitary waves, nematic liquid crystals can support the stable propagation of another type of nonlinear optical beam, the optical vortex, a type of solitary wave with a ring-like structure whose phase increases by an integer multiple n of 2π , the integer n termed the charge of the vortex [3]. The amplitude of the vortex is 0 at its centre to compensate for the phase singularity there. Optical vortices have a number of applications in scientific fields ranging from biology to astronomy [17]. In particular, the amplitude minimum at the centre of the vortex can be used to trap and manipulate small objects, including cells [17]. The behaviour of an optical vortex in a nematic liquid crystal has received much less attention than a nematicon. In a local medium, an optical vortex is unstable to a symmetry breaking azimuthal instability. For the charge 1 vortices to be considered here, the vortex is unstable to a mode 2 azimuthal instability, so that the vortex pinches off at diagonally opposite points and splits into two solitary waves. However, in nonlocal media with sufficiently high nonlocality the nonlocal response can stabilise a charge 1 vortex, but not higher

charge vortices. This instability and restabilisation in nonlocal media has been investigated both numerically [18] and analytically [19]. In a nematic liquid crystal the nonlocal response of the nematic stabilises the vortex due to the optical axis being non-zero in the neighbourhood of the phase singularity [19]. In the local limit of the nematic equations, the optical axis is 0 at the phase singularity, so that the vortex is unstable [19]. Optical vortices have been experimentally generated in nematic liquid crystals, both singly [20, 21], as incoherently interacting pairs [22] and as arrays [23], and in cholesteric liquid crystals [24]. They have also been experimentally generated in colloidal media [25]. The equations governing nonlinear optical beam propagation in colloidal media are similar to those for beam propagation in a nematic liquid crystal [26, 27].

In the present work the refraction of an optical vortex at a nonlinear refractive index interface in a nematic liquid crystal will be investigated using both modulation theory and numerical solutions. The refractive index interface is formed by using two independent external, biasing static electric fields to pre-tilt the nematic molecules at two different angles, as in the experiments of Peccianti *et al* [28]. The experiments of Peccianti *et al* [28] involved the refraction of a nematicon, rather than an optical vortex, but the experimental set-up is the same. While the refraction of a nematicon and an optical vortex have some similarities, they also have distinct differences due to the different stability properties of a nematicon and a vortex. The refraction of a nematicon to a more optically dense medium resembles the equivalent geometric optics refraction of light [28, 29]. However, for the refraction of a nematicon to a less optically dense medium, non-specular total internal reflection regimes exist, which depend on the angle of incidence [28–30]. These include Goos-Hänchen reflection [31], whereby the nematicon enters the less dense medium, but is refracted back and re-enters the original medium, and total internal reflection without impinging on the interface. Both these forms of non-specular reflection are due to a nematicon being an extended object, so that it can have different portions on different sides of the interface. In

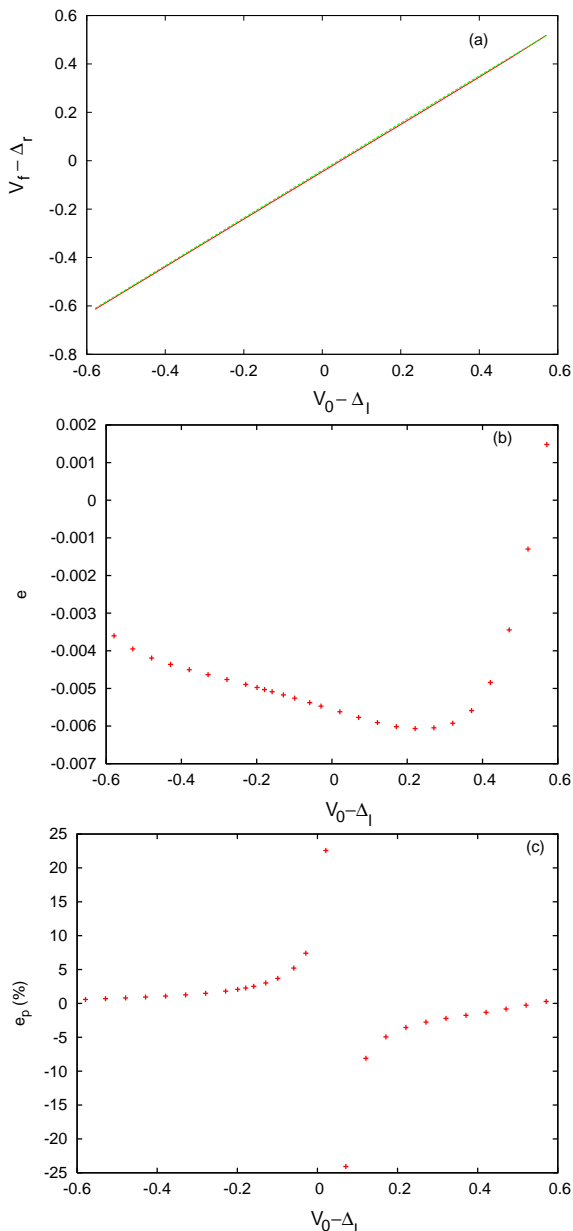


FIG. 1: (Color online) Comparison between full numerical and modulation solutions for the initial values $a = 0.15$ and $w = 8.0$, with $\nu = 200$, $\psi_{bl} = 0.4$, $\psi_{br} = 0.9$, $q_l = 1.0$, $q_r = 1.3$, $\mu_1 = 2$ and $\mu_2 = -80$. (a) Final propagation constant $V_f - \Delta_r$ versus initial value $V_0 - \Delta_l$, numerical solution: — (full red line); modulation solution: - - - (dashed green line), (b) absolute error e between numerical and modulation solutions, (c) percentage error e_p between numerical and modulation solutions.

principle, an optical vortex could also show non-specular reflection at an interface to a less optically dense medium. However, it is shown that the interface triggers the basic mode 2 azimuthal instability of the vortex due to it being in close proximity to the interface for an extended distance for angles of incidence for which non-specular reflection could occur. It is found that the angle of re-

fraction of the vortex as given by modulation theory is in excellent agreement with numerical solutions, for refraction to both more and less optically dense regions. Good agreement for the trajectory is also obtained when the vortex splits into two nematicons. This is found to be due to overall momentum conservation.

II. GOVERNING EQUATIONS AND MODULATION THEORY

Let us consider a planar cell containing a nematic liquid crystal with the boundary condition at the cell walls arranged so that the molecular director, or axis of the nematic molecules, lies in the (x, z) plane. To induce a refractive index change across the nematic two independent, external biasing static electric fields are applied across its thickness [28]. The nematic director can then have two independent orientations measured from the direction z down the cell, resulting in two regions of different refractive index via the nonlinear dependence of the refractive index of the nematic on the director orientation [4, 32]. A coherent beam of light in the form of an optical vortex is then introduced into the cell and propagates down it. To define the coordinate system, let us take the direction of polarisation of the extraordinary light beam and the external electric fields to be in the x direction, which is across the cell thickness. As stated, the z direction is down the cell and the y direction completes the right handed coordinate system. In the paraxial approximation the nondimensional system of equations governing the evolution of the vortex is [4, 5, 32]

$$i \frac{\partial E}{\partial z} - i \Delta \frac{\partial E}{\partial y} + \frac{1}{2} \nabla^2 E + \sin(2\psi_b) \theta E = 0, \quad (1)$$

$$\nu \nabla^2 \theta - 2q\theta = -\sin(2\psi_b) |E|^2. \quad (2)$$

Here E is the complex valued envelope of the electric field of the optical beam. The parameter ν measures the elastic response of the nematic and is large, $O(100)$, in the usual experimental regime [33], so that the response of the nematic is termed nonlocal as it extends far beyond the waist of the beam. The parameter q is proportional to the square of the external biasing electric field [4, 5]. The pre-tilt of the nematic due to the external biasing field is ψ_b . The total angle made by the director to the z direction is $\psi = \psi_b + \theta$. For the usual milliwatt beam power levels [2], the extra rotation caused by the beam is small, $|\theta| \ll |\psi_b|$. As shown in [29], the governing equations (1) and (2) are valid in this small extra deviation limit. Finally, δ is the walk-off angle between the Poynting vector and the wavevector of the extraordinary beam. In the small deviation limit $|\theta| \ll |\psi_b|$ [29]

$$\Delta = \tan \delta = \frac{\Delta n^2 \sin 2\psi_b}{\Delta n^2 + 2n_{\perp}^2 + \Delta n^2 \cos 2\psi_b}, \quad (3)$$

where $\Delta n^2 = n_{\parallel}^2 - n_{\perp}^2$ is the optical birefringence and n_{\parallel} and n_{\perp} are the refractive indices for fields parallel

and perpendicular to the optic axis, respectively [32]. In the present work the typical values $n_{\parallel} = 1.6954$ and $n_{\perp} = 1.5038$ will be used, which are for the nematic E7 at room temperature in the near infrared at wavelength $1.064 \mu\text{m}$ [32, 34]. While the governing equations (1) and (2) have been introduced in the context of nonlinear beam propagation in nematic liquid crystals, they are more general and describe nonlinear wave propagation in a diverse range of media for which nonlinearity is coupled with some diffusive phenomena [35].

The director equation (2) can be solved via a Green's function G to give

$$\theta = -\sin(2\psi_b) \iint_{-\infty}^{\infty} G(x, y, x', y') |E(x', y')|^2 dx' dy', \quad (4)$$

where G is expressed in terms of the modified Bessel function K_0 [19]. The electric field equation (1) then becomes

$$\begin{aligned} i \frac{\partial E}{\partial z} - i\Delta \frac{\partial E}{\partial y} + \frac{1}{2} \nabla^2 E \\ - \sin^2(2\psi_b) E \iint_{-\infty}^{\infty} G(x, y, x', y') |E(x', y')|^2 dx' dy' = 0, \end{aligned} \quad (5)$$

which has the Lagrangian

$$\begin{aligned} L = i(E^* E_z - E E_z^*) - i\Delta(E^* E_y - E E_y^*) - |\nabla E|^2 \\ - \sin^2(2\psi_b) |E|^2 \iint_{-\infty}^{\infty} G(x, y, x', y') |E(x', y')|^2 dx' dy'. \end{aligned} \quad (6)$$

As stated above, the external biasing electric field takes two values across the cell. The same electric field geometry will be used as in the original experiments [28, 36]. We then assume that two different static fields are applied through thin film electrodes separated by a straight gap along the line $z = \mu_1 y + \mu_2$. The electric field, and so the resulting director distribution ψ_b , then has a jump discontinuity along this line. This approximation of a jump in the media properties is in accord with experiments as the electric field was found to vary smoothly between two constant values over a distance of the order of the gap between the electrodes, about $50 \mu\text{m}$ [30, 36]. We then set

$$\psi_b = \begin{cases} \psi_{bl}, & \mu_1 z + \mu_2 < y, \\ \psi_{br}, & y < \mu_1 z + \mu_2 \end{cases} \quad (7)$$

and

$$q = \begin{cases} q_l, & \mu_1 z + \mu_2 < y, \\ q_r, & y < \mu_1 z + \mu_2. \end{cases} \quad (8)$$

As in previous work [19, 37, 38] the electric field will be assumed to be a mode (or charge) one optical vortex of the form

$$E = a r e^{-r/w} e^{i\sigma + iV(y-\xi) + i\phi} + i g e^{i\sigma + iV(y-\xi) + i\phi}. \quad (9)$$

Here $r^2 = x^2 + (y-\xi)^2$ and ϕ is the polar angle relative to the centre of the vortex $(0, \xi)$. The first term in this trial

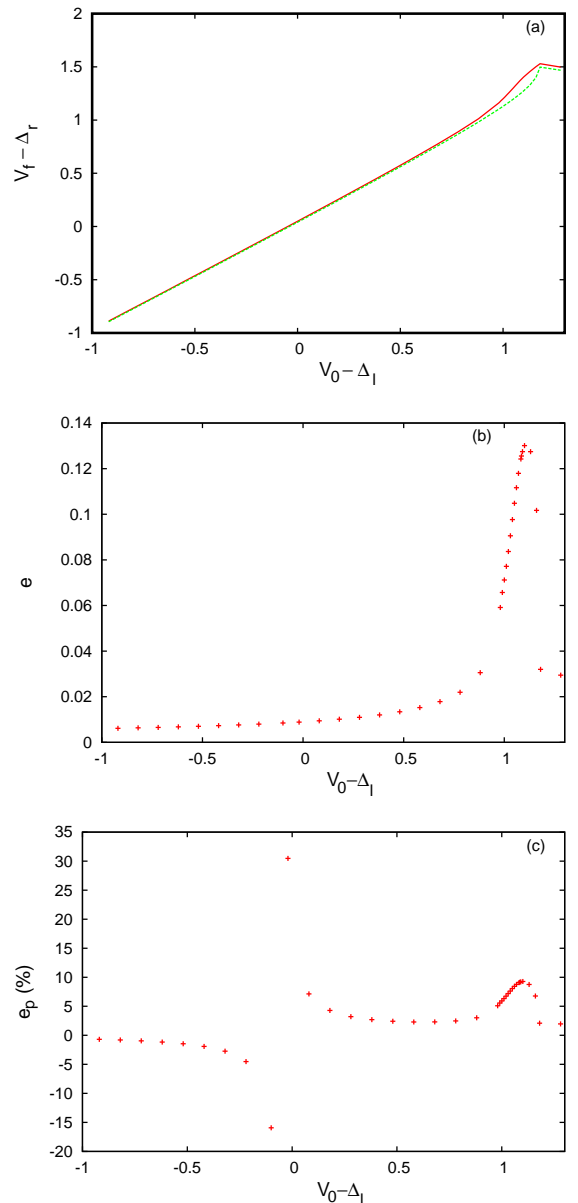


FIG. 2: (Color online) Comparison between full numerical and modulation solutions for the initial values $a = 0.15$ and $w = 8.0$ at $z = 0$, with $\nu = 200$, $\psi_{bl} = 0.8$, $\psi_{br} = 0.4$, $q_l = 1.3$, $q_r = 1.0$, $\mu_1 = 1.5$ and $\mu_2 = -20$. (a) Final propagation constant $V_f - \Delta_r$ versus initial value $V_0 - \Delta_l$, numerical solution: — (full red line); modulation solution: --- (dashed green line), (b) absolute error e between numerical and modulation solutions, (c) percentage error e_p between numerical and modulation solutions.

function is an optical vortex of amplitude $A = a w e^{-1}$ and width w . The second term represents the low wavenumber radiation which accumulates under the vortex as it evolves [19, 39]. Linearising the electric field equation (1) shows that low wavenumber radiation has low group velocity [40], so that low wavenumber radiation accumulates under the vortex. Furthermore, this radiation is

$\pi/2$ out of phase with the vortex as the in-phase component corresponds to changes in the vortex amplitude and width [40]. The low wavenumber radiation forms a shelf of length w under the peak of the vortex, so that g is non-zero in $w/2 \leq r \leq 3w/2$ [19]. The radiation shelf then matches to propagating diffractive radiation, the shedding of which allows the vortex to evolve to a steady state. This shed radiation has a significant effect on the vortex only for large z scales for the nonlocal limit with ν large [39]. As such large propagation distances will not be considered here, the form of this propagating diffractive radiation will not be considered further. A suitable approximation for the director distribution θ is more subtle [19]. The director distribution θ is given by the Green's function solution (4). However, the Green's function kernel involves the modified Bessel function K_0 , so this solution, as it stands, is difficult to use in calculating an averaged Lagrangian from (6). To overcome this difficulty the nonlocal nature of the director response will be used to calculate an asymptotic solution for θ .

As the nonlocality ν is large and the nematic is a non-local medium, relative to the nematic response the vortex in the director equation (2) is a δ function forcing centred at $r = w$ [19, 37, 38]. Furthermore, within the core of the vortex $r \leq w$, the director angle θ is essentially constant, again due to the director response being wide and slowly varying [19, 37, 38]. With these approximations in the nonlocal limit, the director equation (2) can be found to have the asymptotic solution

$$\theta = \begin{cases} \frac{a^2 w^3 \sin(2\psi_b)}{4\sqrt{2q\nu}}, & r < w, \\ \frac{a^2 w^3 \sin(2\psi_b)}{4\sqrt{2q\nu}} e^{-\beta(r-w)}, & r \geq w \end{cases} \quad (10)$$

for ν large, where $\beta = \sqrt{2q/\nu}$.

Now that a suitable approximation to the director distribution has been found, the modulation equations governing the refraction of the vortex can be calculated by averaging the Lagrangian (6) [41]. The averaged Lagrangian and the resulting variational, or modulation equations, are given in Appendix A.

III. COMPARISONS WITH NUMERICAL SOLUTIONS

Results from the developed modulation theory will now be compared with full numerical solutions of the nematic equations governing the vortex. The modulation equations (A2)–(A7) were solved numerically using the standard 4th order Runge-Kutta method. The nematic equations (1) and (2) were solved using the pseudospectral method of Fornberg and Whitham [42]. The only differences with the method of Fornberg and Whitham are that the electric field equation was advanced in z using the 4th order Runge-Kutta method in Fourier, rather than real, space. The sharp interface along $y = \mu_1 z + \mu_2$ can cause spurious oscillations and distortions in the numerical solution. To overcome this the interface, that is

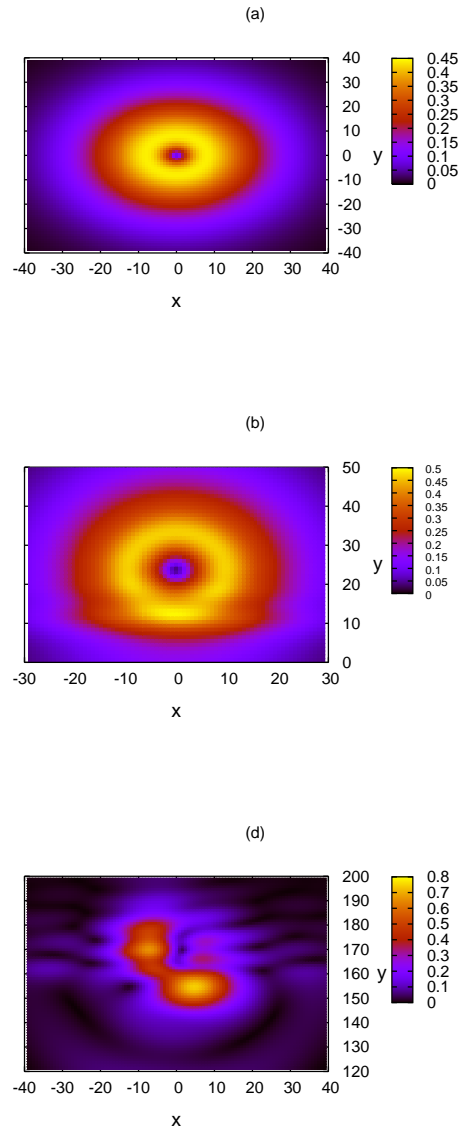


FIG. 3: (Color online) Numerical solution for $|u|$ for the parameter values $a = 0.15$, $w = 8.0$ and $V = 1.3$ at $z = 0$, with $\nu = 200$, $\psi_{bl} = 0.8$, $\psi_{br} = 0.4$, $q_l = 1.3$, $q_r = 1.0$, $\mu_1 = 1.5$ and $\mu_2 = -20$. (a) $z = 0$, (b) $z = 20$, (c) $z = 120$.

ψ_b and q , were smoothed using $\tanh(y - \mu_1 z - \mu_2)/w_t$ to link the orientations ψ_{bl} and ψ_{br} and q_l and q_r on the two sides of the interface. A small width w_t produces a sharp, smooth interface with the numerical solution displaying no spurious effects, the main one of which is an unphysical beam deformation. This smoothing of the interface is in accord with the experimental set-up as the electrodes producing the biasing electric fields were separated by about $50\mu m$, with the electric field varying smoothly between the two constant values over this distance [30, 36]. The numerical y position of the vortex is calculated as

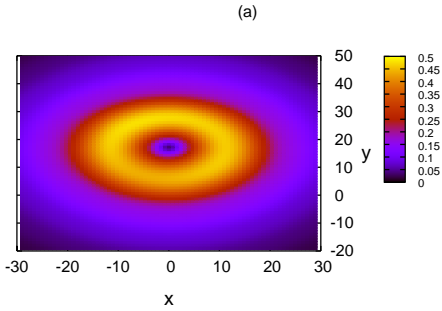


FIG. 4: (Color online) Numerical solution for $|u|$ at $z = 40$ for the parameter values $a = 0.15$, $w = 8.0$ and $V = 0.5$ at $z = 0$, with $\nu = 200$, $\psi_{bl} = 0.8$, $\psi_{br} = 0.4$, $q_l = 1.3$, $q_r = 1.0$, $\mu_1 = 1.5$ and $\mu_2 = -20$.

its centre of mass position

$$\xi = \frac{\int_{-\infty}^{\infty} \int_{-\infty}^{\infty} y |E|^2 dx dy}{\int_{-\infty}^{\infty} \int_{-\infty}^{\infty} |E|^2 dx dy}. \quad (11)$$

Let us first consider refraction to a more optically dense medium. Typical results are shown in Figure 1. This figure shows comparisons between the final propagation constant after the vortex is well past the interface as a function of the initial propagation constant, as given by the full numerical and modulation solutions. Both a direct comparison and the absolute e and percentage errors e_p in the modulation solution are shown. It can be seen that there is excellent agreement between the numerical and modulation solutions, with the error generally being less than 5%. The percentage error e_p becomes large above $V_0 - \Delta_l = 0$ to $V_0 - \Delta_l = 0.1$ as the angle of refraction $V_f - \Delta_r$ is close to 0 and so these errors are being calculated with a small divisor. It can be seen from Figure 1(a) that there is no abrupt change in the comparison between the numerical and modulation solutions in this region and from Figure 1(b), no abrupt change in the absolute error e . On the whole, these results for the refraction of a vortex to a more optically dense medium are similar to those for the refraction of a nematicon (solitary wave) [29]. The change in the angle of propagation across the interface is $O(5^\circ)$, which is the same order as for the refraction of a nematicon [28, 29]. In experiments on nematicons, changes in the angle of propagation of up to 18° were obtained [28]. However, the change in the angle of propagation depends on the jump in the values of ψ and q as these parameters depend on the size of the two pre-tilting electric fields [29, 33].

Let us now consider refraction to a less optically dense medium. The equivalent refraction of a nematicon displays a complicated range of behaviour, depending on the initial propagation angle relative to the interface [28–30, 36]. In addition to the usual refraction to the second medium and total internal reflection of ray theory,

a nematicon can also show Goos-Hänchen reflection [31] whereby its centre refracts into the less dense medium, before re-entering the original medium, and total internal reflection without its centre actually touching the interface. These two latter types of reflection are due to a nematicon not being a point particle, but an extended object, so that when it is close to the interface it can respond to the refractive indices on both sides of it. Figure 2 displays the same propagation constant comparison between the numerical and modulation solutions and the absolute and percentage errors for the modulation results compared with the numerical data as in Figure 1. It can be seen that up to $V_0 - \Delta_l = 0.9$ the agreement between the numerical and modulation solutions is similar to that of Figure 1. Again, for $V_0 - \Delta_l$ between -0.1 and -0.02 the percentage error e_p becomes large due to the angle of refraction $V_f - \Delta_r$ being near 0. Figures 2(a) and (b) show no abrupt change in this range. As for refraction to a more optically dense medium, the change in propagation angle is $O(5^\circ)$, up to about 10° , similar to that for the equivalent refraction of a nematicon [28, 29]. The increasing difference above $V_0 - \Delta_l = 0.9$ is a result of a fundamental difference between a nematicon and an optical vortex, which will now be discussed.

Figure 3 shows numerical solutions for $|u|$ for $V_0 = 1.3$, which gives $V_0 - \Delta_l = 1.1803$, at $z = 0$, $z = 20$ when the vortex reaches the interface at $y = 10$ and $z = 120$ when the beam is still in the vicinity of the interface, which is at $y = 160$. It can be seen from the vortex at $z = 20$ in Figure 3(b) that the interface perturbs the vortex profile, with the solution at $z = 120$ showing that the vortex has been destroyed and has formed two nematicons, solitary waves, with one nematicon on either side of the interface. The equivalent refraction of a nematicon shows no such instability [28, 29]. A charge 1 optical vortex has a mode 2 azimuthal instability if the nonlocality ν is not large enough [18, 19]. This instability pinches off the vortex width in a symmetrical fashion, so that it breaks up into two solitary waves. For a vortex in a uniform medium, if the nonlocality $\nu > 100$, then the vortex is stable against this azimuthal mode [18, 19]. So in a uniform nematic, the vortex of Figure 3 is stable. The destabilising effect of the interface can be seen in Figure 3(b). The interface has perturbed the vortex in a manner broadly similar to a mode 2 azimuthal perturbation. For $V_0 < 1.1$ the vortex refracts through the interface and does not stay close to it for a long range of z . However, for $V_0 > 1.1$ the vortex is close to total internal reflection and propagates close to the interface for an extended range of z . This close proximity to the boundary for an extended range of z forces the unstable azimuthal mode long enough to cause the vortex to become unstable and split into two nematicons, as in Figure 3(c). A contrary example for $V_0 = 0.5$ of a vortex refracting through the interface and remaining stable is shown in Figure 4, which shows the vortex well after it has passed through the interface, which is at $y = 40$ at $z = 40$. The vortex has returned to a uniform state and resembles the initial vortex shown in Figure

3(a).

In the non-paraxial approximation a similar effect due to close proximity at a low angle of incidence relative to a refractive index interface for an extended distance occurs for the refraction of solitary waves [43]. In this work, the change in nonlinear refractive index was chosen so that the solitary wave broke up into multiple solitary waves after refraction. It was found that a non-paraxial solitary wave breaks up into more solitary waves than predicted by paraxial theory when the angle of incidence was low, so that the incident solitary wave propagates close to the interface for an extended distance. The actual stability analysis of the current interface effect for a vortex would be non-trivial as the related eigenvalue problem would be non-autonomous. Due to this inherent instability of a vortex, Goos-Hänchen reflection and total internal reflection, as seen in the refraction of a nematicon [28, 29], will not occur. The trial function (9) does not include dependence on the polar angle ϕ and so cannot fully capture the instability mechanism of the vortex [19, 37, 38]. However, for $V > 1.18$ the modulation equations show instability. The modulation amplitude shows a large oscillation as it approaches the interface, which corresponds to the vortex width becoming small, after which the amplitude goes to 0. The small vortex width is mimicking the pinching off of the width vortex instability [19]. The modulation analysis then captures the essentials of the instability of the vortex due to the boundary with the critical value $V = 1.18$ for instability in excellent agreement with the numerical value of $V = 1.1$.

Remarkably, Figures 2(b) and 2(c) show that even when the vortex splits into two nematicons, the modulation theory position is still in good agreement with the numerical centre of mass position (11), with the percentage difference e_p only going up to $\sim 10\%$. This is due to overall momentum conservation and shows that when the vortex splits, it does not shed much mass and momentum into diffractive radiation. Experiments with nematicons obtained changes in angles of propagation of up to 22° for propagation into a less optically dense nematic [28], greater than the 10° obtained here. However, these larger angles were for the case of total internal reflection, for which the vortex is unstable. Furthermore, as for refraction to a more optically dense medium, the change in angle depends on the voltage difference of the pre-tilting electric fields, and so on the changes in the values of ψ and q . Finally, in principle, increasing the nonlocality should stabilise the vortex. However, even an unrealistically large value $\nu = 1000$ did not stop the vortex breaking up into nematicons.

IV. CONCLUSIONS

The refraction of an optical vortex at an interface between two regions of different refractive index in a nematic liquid crystal has been investigated using both modulation theory and full numerical solutions of the

governing equations. A nematic liquid crystal is a specific example of a nonlinear, nonlocal optical medium and the results obtained here would transfer over to other such media [35, 44]. The refraction of a vortex displays distinct behaviour, depending on whether it propagates into a more or less optically dense medium. Refraction to a more optically dense medium is similar to the equivalent refraction of a nematicon [28, 29]. As for the refraction of a nematicon, excellent agreement was found between modulation theory results and numerical solutions, with the change in propagation angle of the vortex being similar to that for a nematicon.

Refraction of a vortex to a less optically dense medium shows major differences to the equivalent refraction of a nematicon [28, 29]. Unlike a nematicon (solitary wave), an optical vortex has an unstable azimuthal mode, which can be triggered if the vortex propagates for too far too close to the interface. In a related context, it has been found that if an optical vortex in a nematic liquid crystal cell propagates too close to the cell walls it can become unstable, even if the nonlocality is large enough so that it is stable away from the boundary [45, 46]. However, this effect is different to that investigated here in that as it is the non-zero value of the optical axis perturbation under the vortex which stabilises it, the cell walls destabilise the vortex as, due to the anchoring conditions, the optical axis is fixed there. In the present context, the vortex is an extended structure and can have portions on both sides of the interface. The resulting shape perturbation can then trigger its azimuthal instability.

Optical vortices are inherently less stable structures than optical solitary waves, nematicons. It is then of interest to study the behaviour and stability of optical vortices in nematic cells with varying properties and refractive index [7–15, 33, 47]. Such variations in refractive index in a cell are the basis for proposed applications of nonlinear optical beams in liquid crystals as they allow the trajectory of the beam to be controlled.

Appendix A: Modulation Equations

The trial function (9) for the electric field and the Green's function solution (4) for θ , based on the approximation (10), are now substituted into the Lagrangian (6). Integrating in x and y from $-\infty$ to ∞ , that is averaging,

yields the averaged Lagrangian [41]

$$\begin{aligned}
\mathcal{L} = & -4 \left(\frac{3}{8} a^2 w^4 + \Lambda_1 g^2 \right) \left(\sigma' - V \xi' + \frac{1}{2} V^2 \right) \\
& - 8aw^3 g' + 8w^3 ga' + 24aw^2 gw' - \frac{3}{4} a^2 w^2 - 2\Lambda_2 g^2 \\
& + A_1^4 V a^2 w^4 [\Delta_l \operatorname{erfc}(\lambda_l) + \Delta_r \operatorname{erfc}(-\lambda_l) \\
& + \frac{\lambda_1}{\sqrt{\pi}} (\Delta_l - \Delta_r) e^{-\lambda_1^2}] \\
& + \sin^2(2\psi_{bl}) \frac{3a^4 w^3 e^{\beta_l w}}{2\sqrt{2q_l\nu}} \left(\beta_l + \frac{2}{w} \right)^{-4} \times \\
& \left[\operatorname{erfc}(\lambda_l) + \frac{\lambda_l}{\sqrt{\pi}} e^{-\lambda_l^2} \right] \\
& + \sin^2(2\psi_{br}) \frac{3a^4 w^3 e^{\beta_r w}}{2\sqrt{2q_r\nu}} \left(\beta_r + \frac{2}{w} \right)^{-4} \times \\
& \left[\operatorname{erfc}(-\lambda_r) - \frac{\lambda_r}{\sqrt{\pi}} e^{-\lambda_r^2} \right].
\end{aligned} \tag{A1}$$

Taking variations of this averaged Lagrangian with respect to the vortex parameters yields the variational, or modulation equations, for the evolution of the vortex

$$\frac{d}{dz} \left[\frac{3}{8} a^2 w^4 + \Lambda_1 g^2 \right] = 0, \tag{A2}$$

$$4 \frac{d}{dz} (aw^3) = 2\Lambda_1 g \left[\sigma' - V \xi' + \frac{1}{2} V^2 \right] + \Lambda_2 g, \tag{A3}$$

$$\frac{d\xi}{dz} = V - \frac{1}{2} [\Delta_l \operatorname{erfc}(\lambda_l) + \Delta_r \operatorname{erfc}(-\lambda_l) + \frac{\lambda_1}{\sqrt{\pi}} (\Delta_l - \Delta_r) e^{-\lambda_1^2}], \tag{A4}$$

$$\begin{aligned}
4 \frac{d}{dz} \left[\frac{3}{8} a^2 w^4 + \Lambda_1 g^2 \right] V = & \frac{A_1^3}{\sqrt{\pi}} a^2 w^3 V (\Delta_l - \Delta_r) (1 + 2\lambda_1^2) e^{-\lambda_1^2} \\
& - \sin^2(2\psi_{bl}) \frac{a^4 w^3 e^{\beta_l w - \lambda_l^2}}{4A_2^3 \sqrt{2\pi q_l \nu}} \left(\beta_l + \frac{2}{w} \right)^{-3} \times \\
& \left(\frac{1}{2} + \lambda_l^2 \right) \\
& + \sin^2(2\psi_{br}) \frac{a^4 w^3 e^{\beta_r w - \lambda_r^2}}{4A_2^3 \sqrt{2\pi q_r \nu}} \left(\beta_r + \frac{2}{w} \right)^{-3} \times \\
& \left(\frac{1}{2} + \lambda_r^2 \right),
\end{aligned} \tag{A5}$$

$$\begin{aligned}
\frac{dg}{dz} = & \frac{3}{32} \frac{a}{w} + \frac{3\lambda_1 V a w}{64\sqrt{\pi}} (\Delta_l - \Delta_r) (1 + 2\lambda_1^2) e^{-\lambda_1^2} \\
& + \sin^2(2\psi_{bl}) \frac{3a^3 e^{\beta_l w}}{32w\sqrt{2q_l\nu}} \left(\beta_l + \frac{2}{w} \right)^{-5} \times \\
& \left[\frac{1}{\sqrt{\pi}} (\beta_l^2 w^2 - 3\beta_l w + 4\lambda_l^2) \lambda_l e^{-\lambda_l^2} \right. \\
& \left. - (2 + 3\beta_l w - \beta_l^2 w^2) \operatorname{erfc}(\lambda_l) \right] \\
& - \sin^2(2\psi_{br}) \frac{3a^3 e^{\beta_r w}}{32w\sqrt{2q_r\nu}} \left(\beta_r + \frac{2}{w} \right)^{-5} \times \\
& \left[\frac{1}{\sqrt{\pi}} (\beta_r^2 w^2 - 3\beta_r w + 4\lambda_r^2) \lambda_r e^{-\lambda_r^2} \right. \\
& \left. + (2 + 3\beta_r w - \beta_r^2 w^2) \operatorname{erfc}(-\lambda_r) \right],
\end{aligned} \tag{A6}$$

$$\begin{aligned}
\frac{d\sigma}{dz} - V \frac{d\xi}{dz} + \frac{1}{2} V^2 = & -w^{-2} \\
& + \frac{1}{4} V [2\Delta_l \operatorname{erfc}(\lambda_l) + 2\Delta_r \operatorname{erfc}(-\lambda_l) \\
& + \frac{1}{\sqrt{\pi}} (\Delta_l - \Delta_r) (1 - 2\lambda_1^2) \lambda_1 e^{-\lambda_1^2}] \\
& + \sin^2(2\psi_{bl}) \frac{a^2 e^{\beta_l w}}{2w^2 \sqrt{2q_l\nu}} \left(\beta_l + \frac{2}{w} \right)^{-5} \times \\
& \left[\frac{1}{\sqrt{\pi}} (8 + 7\beta_l w - \beta_l^2 w^2 - 4\lambda_l^2) \lambda_l e^{-\lambda_l^2} \right. \\
& \left. + (10 + 7\beta_l w - \beta_l^2 w^2) \operatorname{erfc}(\lambda_l) \right] \\
& - \sin^2(2\psi_{br}) \frac{a^2 e^{\beta_r w}}{2w^2 \sqrt{2q_r\nu}} \left(\beta_r + \frac{2}{w} \right)^{-5} \times \\
& \left[\frac{1}{\sqrt{\pi}} (8 + 7\beta_r w - \beta_r^2 w^2 - 4\lambda_r^2) \lambda_r e^{-\lambda_r^2} \right. \\
& \left. - (10 + 7\beta_r w - \beta_r^2 w^2) \operatorname{erfc}(-\lambda_r) \right]
\end{aligned} \tag{A7}$$

Here

$$\begin{aligned}
\Lambda_1 = & w^2, \quad \Lambda_2 = \ln 3, \\
\beta_l = & \sqrt{\frac{2q_l}{\nu}}, \quad \beta_r = \sqrt{\frac{2q_r}{\nu}}, \quad \lambda_1 = \frac{\mu_1 z + \mu_2 - \xi}{A_1 w}, \\
\lambda_l = & A_2 \left(\beta_l + \frac{2}{w} \right) (\mu_1 z + \mu_2 - \xi), \\
\lambda_r = & A_2 \left(\beta_r + \frac{2}{w} \right) (\mu_1 z + \mu_2 - \xi), \\
A_1 = & \left(\frac{3}{4} \right)^{1/4}, \quad A_2 = 12^{-1/4}.
\end{aligned} \tag{A8}$$

The modulation equation (A2) is the equation for conservation of optical power and (A5) is that for conservation of y momentum [48]. As the vortex evolves it will shed diffractive radiation [39]. However, as for the refraction of a nematicon, this shed radiation is not significant over the z distances considered here. It should be noted that to calculate the integrals in the averaged Lagrangian involving θ the expression for θ in (10) for $r > w$ was

extended into $r < w$. This is a valid approximation for large ν as the error involved is $O(\nu^{-1})$. Without this ap-

proximation, the integrals could not be evaluated due to the change across $z = \mu_1 y + \mu_2$.

-
- [1] G. Assanto, M. Peccianti and C. Conti, "Optical spatial solitons in nematic liquid crystals. Nematicons," *Optics & Photonic News* **14**, 45–48 (2003).
- [2] M. Peccianti, A. De Rossi, G. Assanto, A. De Luca, C. Umeton, and I.C. Khoo, "Electrically assisted self-confinement and waveguiding in planar nematic liquid crystal cells," *Appl. Phys. Lett.*, **77**, 7–9 (2000).
- [3] Yu.S. Kivshar and G. Agrawal, *Optical Solitons: From Fibers to Photonic Crystals*, Academic Press, San Diego, (2003).
- [4] C. Conti, M. Peccianti and G. Assanto, "Route to nonlocality and observation of accessible solitons," *Phys. Rev. Lett.*, **91**, 073901 (2003).
- [5] C. Conti, M. Peccianti and G. Assanto, "Observation of optical spatial solitons in a highly nonlocal medium," *Phys. Rev. Lett.*, **92**, 113902 (2004).
- [6] G. Assanto, A.A. Minzoni and N.F. Smyth, "Light self-localization in nematic liquid crystals: modelling solitons in nonlocal reorientational media," *J. Nonlin. Opt. Phys. and Mater.*, **18**, 657–691 (2009).
- [7] M. Peccianti, C. Conti, G. Assanto, A. de Luca and C. Umeton, "All-optical switching and logic gating with spatial solitons in liquid crystals," *Appl. Phys. Lett.*, **81**, 3335–3337 (2002).
- [8] S.V. Serak, N.V. Tabiryan, M. Peccianti and G. Assanto, "Spatial soliton all-optical logic gates" *IEEE Photon. Tech. Lett.*, **18**, 1287–1289 (2006).
- [9] M. Peccianti, A. Dyadyusha, M. Kaczmarek and G. Assanto, "Escaping solitons from a trapping potential," *Phys. Rev. Lett.*, **101**, 153902 (2008).
- [10] A. Piccardi, G. Assanto, L. Lucchetti and F. Simoni, "All-optical steering of soliton waveguides in dye-doped liquid crystals," *Appl. Phys. Lett.* **93**, 171104 (2008).
- [11] G. Assanto, A. Piccardi, A. Alberucci, S. Residori and U. Bortolozzo, "Liquid crystal light valves: a versatile platform for nematicons," **1**, 151–153 (2009).
- [12] G. Assanto, B.D. Skuse and N.F. Smyth, "Optical path control of spatial optical solitary waves in dye-doped nematic liquid crystals," *Photon. Lett. Poland*, **1**, pp. 154–156 (2009).
- [13] A. Alberucci, A. Piccardi, U. Bortolozzo, S. Residori and G. Assanto, "Nematicon all-optical control in liquid crystal light valves," *Opt. Lett.*, **35**, 390–392 (2010).
- [14] A. Piccardi, A. Alberucci, U. Bortolozzo, S. Residori and G. Assanto, "Soliton gating and switching in liquid crystal light valve," *Appl. Phys. Lett.*, **96**, 071104 (2010).
- [15] G. Assanto, B.D. Skuse and N.F. Smyth, "Solitary wave propagation and steering through light-induced refractive potentials," *Phys. Rev. A*, **81**, 063811 (2010).
- [16] M. Peccianti, C. Conti, G. Assanto, A. de Luca and C. Umeton, "Routing of anisotropic spatial solitons and modulational instability in liquid crystals," *Nature*, **432**, 733–737 (2004).
- [17] D.L. Andrews, *Structured Light and Its Applications: An Introduction to Phase-Structured Beams and Nanoscale Optical Forces*, Academic Press-Elsevier, Burlington, (2008).
- [18] A.I. Yakimenko, Yu.A. Zaliznyak and Yu.S. Kivshar, "Stable vortex solitons in nonlocal self-focusing nonlinear media," *Phys. Rev. E*, **71**, 065603(R) (2005).
- [19] A.A. Minzoni, N.F. Smyth, A.L. Worthy and Y.S. Kivshar, "Stabilization of vortex solitons in nonlocal nonlinear media," *Phys. Rev. A*, **76**, 063803 (2007).
- [20] E. Brasselet, N. Murazawa, H. Misawa and S. Juodkazis, "Optical vortices from liquid crystal droplets," *Phys. Rev. Lett.*, **103**, 103903 (2009).
- [21] E. Brasselet and C. Loussert, "Electrically controlled topological defects in liquid crystals as tunable spin-orbit encoders for photons," *Opt. Lett.* **36**, 719–721 (2011).
- [22] Y.V. Izdebskaya, J. Rebling, A.S. Desyatnikov and Y.S. Kivshar, "Observation of vector solitons with hidden vorticity," *Opt. Lett.*, **37**, 767–769 (2012).
- [23] E. Brasselet, "Tunable optical vortex arrays from a single nematic topological defect," *Phys. Rev. Lett.*, **108**, 087801 (2012).
- [24] D. Voloschenko and O.D. Lavrentovich, "Optical vortices generated by dislocations in a cholesteric liquid crystal," *Opt. Lett.*, **25**, 317–319 (2000).
- [25] M.P. MacDonald, P. Prentice and K. Dholakia, "Optical vortices produced by diffraction from dislocations in two-dimensional colloidal crystals," *New J. Phys.*, **8**, 257 (2006).
- [26] M. Matuszewski, W. Krolikowski and Y. S. Kivshar, "Spatial solitons and light-induced instabilities in colloidal media," *Opt. Exp.*, **16**, 1371–1376 (2008).
- [27] M. Matuszewski, W. Krolikowski and Y. S. Kivshar. "Soliton interactions and transformations in colloidal media." *Phys. Rev. A*, **79**, 023814 (2009).
- [28] M. Peccianti, A. Dyadyusha, M. Kaczmarek and G. Assanto, "Tunable refraction and reflection of self-contained light beams," *Nature Phys.*, **2**, 737–742 (2006).
- [29] G. Assanto, N.F. Smyth and W. Xia, "Modulation analysis of nonlinear beam refraction at an interface in liquid crystals," *Phys. Rev. A*, **84**, 033818 (2011).
- [30] M. Peccianti, G. Assanto, A. Dyadyusha and M. Kaczmarek, "Nonspecular total internal reflection of spatial soliton at the interface between highly birefringent media," *Phys. Rev. Lett.*, **98**, 113902 (2007).
- [31] F. Goos and H. Hänchen, "Ein neuer und fundamentaler Versuch zur Totalreflexion," *Ann. Phys.*, **436**, 333–346 (1947).
- [32] M. Peccianti, A. Fratolocchi and G. Assanto, "Transverse dynamics of nematicons," *Opt. Express*, **12**, 6524–6529 (2004).
- [33] G. Assanto, A.A. Minzoni, M. Peccianti and N.F. Smyth, "Optical solitary waves escaping a wide trapping potential in nematic liquid crystals: modulation theory," *Phys. Rev. A*, **79**, 033837 (2009).
- [34] *CRC Handbook of Laser Science and Technology: Optical Materials*, Suppl. 2, ed. M.J. Weber, CRC Press, New York (1995).
- [35] A.B. Aceves, J.V. Moloney and A.C. Newell, "Theory of light-beam propagation at nonlinear interfaces. I Equivalent-particle theory for a single interface," *Phys.*

- Rev. A*, **39**, 1809–1827 (1989).
- [36] M. Peccianti, G. Assanto, A. Dyadyusha and M. Kuczmarek, “Nonlinear shift of spatial solitons at a graded dielectric interface,” *Opt. Lett.*, **32**, 271–273 (2007).
- [37] Z. Xu, N.F. Smyth, A.A. Minzoni and Y.S. Kivshar, “Vector vortex solitons in nematic liquid crystals,” *Opt. Lett.*, **34**, 1414–1416 (2009).
- [38] A.A. Minzoni, N.F. Smyth, Z. Xu and Y.S. Kivshar, “Stabilization of vortex-soliton beams in nematic liquid crystals,” *Phys. Rev. A*, **79**, 063808 (2009).
- [39] A.A. Minzoni, N.F. Smyth and A.L. Worthy, “Modulation solutions for nematicon propagation in non-local liquid crystals,” *J. Opt. Soc. Amer. B*, **24**, pp. 1549–1556 (2007).
- [40] W.L. Kath and N.F. Smyth, “Soliton evolution and radiation loss for the nonlinear Schrödinger equation,” *Phys. Rev. E*, **51**, 1484–1492 (1995).
- [41] G.B. Whitham, *Linear and Nonlinear Waves*, J. Wiley and Sons, New York (1974).
- [42] B. Fornberg and G.B. Whitham, “A numerical and theoretical study of certain nonlinear wave phenomena,” *Phil. Trans. R. Soc. Lond. A*, **289**, 373–403 (1978).
- [43] J. Sánchez-Curto, P. Chamarro-Posada and G.S. McDonald, “Helmholtz bright and dark soliton splitting at nonlinear interfaces,” *Phys. Rev. A*, **85**, 013836 (2012).
- [44] A.B. Aceves, P. Varatharajah, A.C. Newell, E.M. Wright, G.I. Stegeman, D.R. Heatley, J.V. Moloney and H. Adachihara, “Particle aspects of collimated light channel propagation at nonlinear interfaces and in waveguides,” *J. Opt. Soc. Amer. B*, **7**, 963–974 (1990).
- [45] A.A. Minzoni, N.F. Smyth and Z. Xu, “Stability of an optical vortex in a circular nematic cell,” *Phys. Rev. A*, **81**, 033816 (2010).
- [46] Y.V. Izdebskaya, A.S. Desyatnikov, G. Assanto and Y.S. Kivshar, “Dipole azimuthons and vortex charge flipping in nematic liquid crystals,” *Opt. Expr.*, **19**, 21457–21466 (2011).
- [47] G. Assanto, A.A. Minzoni, N.F. Smyth and A.L. Worthy, “Refraction of nonlinear beams by localised refractive index changes in nematic liquid crystals,” *Phys. Rev. A*, **82**, 053843 (2010).
- [48] D.J. Kaup and A.C. Newell, “Solitons as particles, oscillators, and in slowly changing media: a singular perturbation theory,” *Proc. Roy. Soc. Lond. A*, **361**, 413–446 (1978).